JOURNAL OF MATERIALS SCIENCE 11 (1976) 500–509

Thermodynamics and kinetics of oxidation of hot-pressed silicon nitride

S. C. SINGHAL
Materials Science Section, Metallurgy and Metals Processing Department, Westinghouse Research Laboratories, Pittsburgh, Pennsylvania, USA

The "passive" oxidation behaviour of silicon nitride hot-pressed with 1 wt % MgO has been studied in dry oxygen in the temperature range 1000 to 1400° C. The oxidation follows the classical parabolic behaviour with an apparent activation energy of 375 kJ mol^{-1}. Except for minor amounts of a glass and cristobalite, the oxide film consists predominantly of $MgSiO_3$ in which various impurity elements, e.g. Ca, Fe, Al, etc., concentrate. The outward diffusion of Mg^{2+} and impurity cations from the grain-boundary glass phase through the oxide film appears to be oxidation rate controlling.

1. Introduction

The recent interest [1, 2] in hot-pressed silicon nitride for potential application as a structural material in gas turbines at high temperatures has prompted the need for an understanding of its oxidation behaviour. Although several studies have been reported on the oxidation of powdered [3-5] and reaction-sintered [6] silicon nitride, no comprehensive investigation of the oxidation behaviour of dense hot-pressed silicon nitride has previously been carried out.

Similar to Si and SiC, silicon nitride can have two distinct types of oxidation behaviour at high temperatures depending upon the ambient oxygen potential. At high oxygen potentials, a thin protective film of $SiO_2(s)$ is formed according to reaction:

$$Si_3N_4(s) + 3O_2 \rightarrow 3SiO_2(s) + 2N_2 \quad (1)$$

although in some cases, silicon oxynitride (Si_2ON_2) may form as an intermediate phase. The formation of $SiO_2(s)$ film in this "passive" oxidation of silicon nitride limits the rate of further oxidation. As opposed to this "passive" oxidation in highly oxidizing atmospheres, severe "active" oxidation can occur at low oxygen potentials according to reactions:

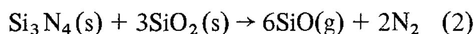

$$Si_3N_4(s) + 3SiO_2(s) \rightarrow 6SiO(g) + 2N_2 \quad (2)$$

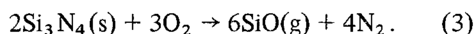

$$2Si_3N_4(s) + 3O_2 \rightarrow 6SiO(g) + 4N_2. \quad (3)$$

This "active" oxidation is characterized by a loss in weight during oxidation due to the formation of gaseous silicon monoxide (SiO). Using Wagner's theoretical model [7], it is calculated [8] that this "active" oxidation of Si_3N_4 will occur only at oxygen partial pressures less than $\sim 8 \times 10^{-4}$ atm at 1600 K. The purpose of this paper is to report only on the "passive" oxidation behaviour of commercially-available hot-pressed silicon nitride in 1 atm oxygen in the temperature range 1000 to 1400° C, and to analyse the oxidation data in terms of the various phases reported in the silicon–nitrogen–oxygen system.

2. Experimental

2.1. Material

Silicon nitride used in this investigation was commercially* obtained in the form of ~2.5 cm thick billets. The material had a finished density greater than 99.9% theoretical density. The material contained about 1% MgO which is intentionally added during hot-pressing to obtain near-theoretical density high strength silicon nitride. The material also contained minor amounts of Ca, Fe, Al, Na, K and Mn as shown in the spectrographic chemical analysis of the material in Table I. In addition, the hot-pressed Si_3N_4 contained up to 3 wt % tungsten in the form of tungsten carbide.

A detailed microstructural characterization of this material has been given by Kossowsky [9].

* Grade HS-130, Norton Company, Worcester, MA.

© 1976 Chapman and Hall Ltd. Printed in Great Britain.

TABLE I Emission spectrographic analysis of Si_3N_4

Element	wt %	Element	wt %
Mg	0.8	Mn	0.03
Fe	0.6	Na	0.004
Al	0.1	K	0.003
Ca	0.07	W	~ 3
Cr	0.04	Si	major

The X-ray diffraction analysis of the material revealed the presence of only β–Si_3N_4 with traces of Si_2ON_2. In addition, Kossowsky reported that Mg, Ca, Na and K concentrate in a grain-boundary glass phase of approximate composition, CaO.MgO. $8SiO_2$.

2.2. Experimental procedure

The oxidation experiments were carried out by continuous thermogravimetry using an automatic Cahn electrobalance with a sensitivity of 2 μg. The silicon nitride samples in the form of 1 cm square and 0.2 cm thick plates were cut from the hot-pressed billets and polished with up to 6 μm diamond paste. The polished specimen was suspended from the balance with a sapphire fibre and held in the hot zone of a platinum-resistance furnace in a flowing oxygen atmosphere. The changes in the weight of the specimen were continuously recorded on a strip chart recorder.

Most oxidation experiments were carried out in dry oxygen at 1 atm pressure (1.01×10^5 Pa). The oxygen gas was dried by passing through anhydrous calcium silicate and phosphorus pentoxide before passing it over the specimen suspended from the balance.

In order to study the effect, if any, of the oxygen partial pressure on the "passive" oxidation of Si_3N_4, thermogravimetric experiments were conducted at 1370° C in O_2–Ar gas mixtures with oxygen partial pressures of 0.01, 0.05, 0.1, 0.3, 0.5, 0.7 and 0.9 atm at a total pressure of 1 atm. Similarly, in order to study the effect of nitrogen partial pressure on the oxidation kinetics of hot-pressed Si_3N_4, experiments were conducted using N_2–O_2–Ar gas mixtures with varying nitrogen partial pressures, 0.1, 0.2, 0.3, 0.4, 0.5, 0.6 and 0.7 atm at a fixed oxygen partial pressure (0.2 atm) and fixed total pressure (1 atm).

After oxidation, the surfaces of the specimens were analysed by X-ray diffraction, scanning electron microscopy and electron microprobe analysis to completely characterize the oxidation products formed at different temperatures.

3. Results

3.1. Effect of oxygen flow rate

The initial oxidation experiments were performed at different flow rates of oxygen from 500 to 5000 ml min^{-1}, for which the gas velocities in the reaction tube (~ 2 cm diameter) ranged between 2.6 to 26 cm sec^{-1}. The oxidation rates were found to be independent of the oxygen flow rate at all temperatures in the range 1000 to 1400° C, indicating that the oxidation of Si_3N_4 was not controlled by gas transport in the surface boundary layer. Flow rate in all subsequent oxidation experiments was maintained at 500 ml min^{-1}.

3.2. Effect of temperature

The weight change data for oxidation of Si_3N_4 in 1 atm dry oxygen at different temperatures are summarized in Fig. 1. No detectable weight gain was observed for oxidation at 1000° C and below.

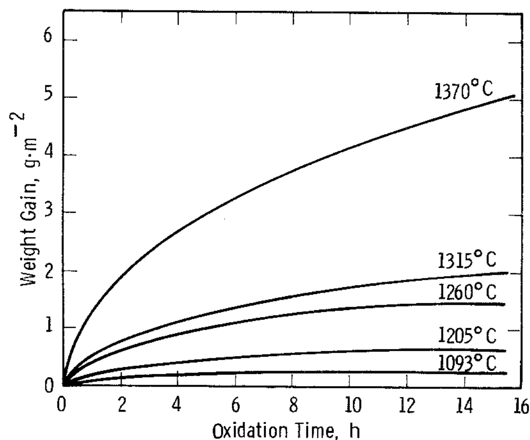

Figure 1 Weight change versus time curves for hot-pressed Si_3N_4 in dry oxygen at 1 atm pressure.

The weight gain versus time curves at all temperatures approximate the classical parabolic behaviour, which can be represented by the equation:

$$W^2 = K_p \cdot t$$

where W is the weight gain at time t, and K_p is the parabolic rate constant. Plots of the square of the weight gain (W^2) as a function of time (t) for different temperatures of oxidation are shown in Fig. 2, where the straight lines represent a region of parabolic oxidation behaviour.

The parabolic rate constants (K_p) for the oxidation of silicon nitride, obtained from the slopes of the straight lines in Fig. 2, are shown in Fig. 3 as a function of temperature. Using the Arrhenius

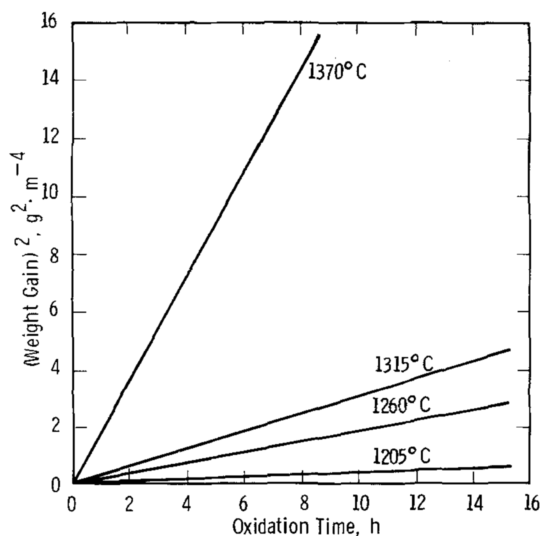

Figure 2 Parabolic plots for oxidation of hot-pressed Si_3N_4 in oxygen at 1 atm pressure.

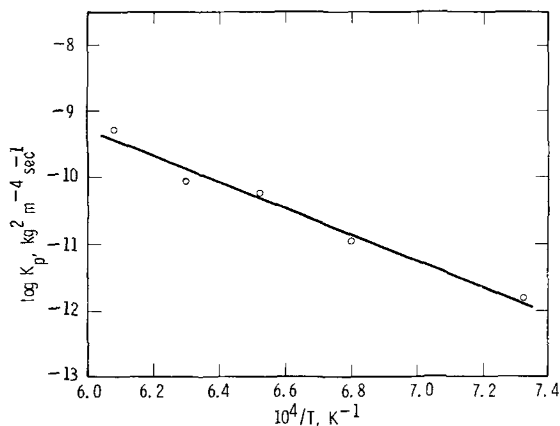

Figure 3 Parabolic rate constants for oxidation of hot-pressed Si_3N_4 in oxygen at 1 atm pressure as a function of temperature.

equation:

$$K_p = A \exp(-E/RT)$$

where E is the activation energy, R is the gas constant and T the absolute temperature, an activation energy of 375 kJ mol^{-1} is obtained for the oxidation of hot-pressed Si_3N_4 in 1 atm oxygen in the temperature range 1000 to 1400° C.

3.3. Effect of oxygen and nitogen partial pressures

The weight gain versus time curves for oxidation of Si_3N_4 at 1370° C in O_2–Ar gas mixtures with oxygen partial pressures from 0.01 to 0.9 atm were identical to those obtained in pure oxygen. Similarly, the weight gain versus time curves for oxidation in N_2–O_2–Ar gas mixtures were identical to those obtained in pure oxygen. Also, the oxidation products formed in these gas mixtures were similar to those obtained in pure oxygen. Even though the range of oxygen and nitrogen partial pressures used was quite small, it indicates that the oxidation rate of hot-pressed Si_3N_4, within the "passive" oxidation region, is independent of ambient oxygen and nitrogen partial pressures.

3.4. Characterization of oxidation products

The surface morphologies of the oxide films formed on Si_3N_4 after oxidation in pure oxygen for 30 h at various temperatures are shown in the scanning electron micrographs in Fig. 4. The oxide formed at 982° C is completely glassy and severely cracked. At 1093° C, a long needle-like crystalline phase, inferred to be mainly enstatite ($MgSiO_3$) by energy dispersive X-ray analysis, starts to appear. The amount of this needle-like phase increases with increasing temperature of oxidation, and at 1305 and 1370° C, the surface is completely covered with this enstatite phase. In addition to this needle-like enstatite phase, the surfaces of the oxidized specimens appear to contain another phase, most probably cristobalite (SiO_2) as identified later by X-ray diffraction analysis.

The scanning electron micrograph of a tranverse section of a Si_3N_4 specimen oxidized for 30 h at 1260° C is shown in Fig. 5 along with the energy dispersive X-ray scans in both Si_3N_4 substrate and the oxide film thereon. While only silicon peak could be detected in the unoxidized Si_3N_4 substrate, peaks representing Mg, Al, Ca, Fe, Mn, Na and K were also easily located in the scan on the oxide film.* These elements evidently concentrate in the oxide film during the oxidation process. The concentration of these elements in the oxide film was confirmed by scanning X-ray pictures shown in Fig. 6, which were taken on oxidized Si_3N_4 surfaces using an electron beam microprobe analyser. Although, these microprobe pictures are shown for oxidation products formed at only 1260° C, similar behaviour was observed at all oxidation temperatures in the range 1100 to 1400° C.

The identity of the oxidation products formed at various temperatures was established by taking X-ray Debye–Scherrer patterns of the surface

* The Au and Pd peaks in the scan are from the surface film of an Au–Pd alloy deposited on oxidized silicon nitride specimen to obtain a conducting surface for scanning electron microscopy.

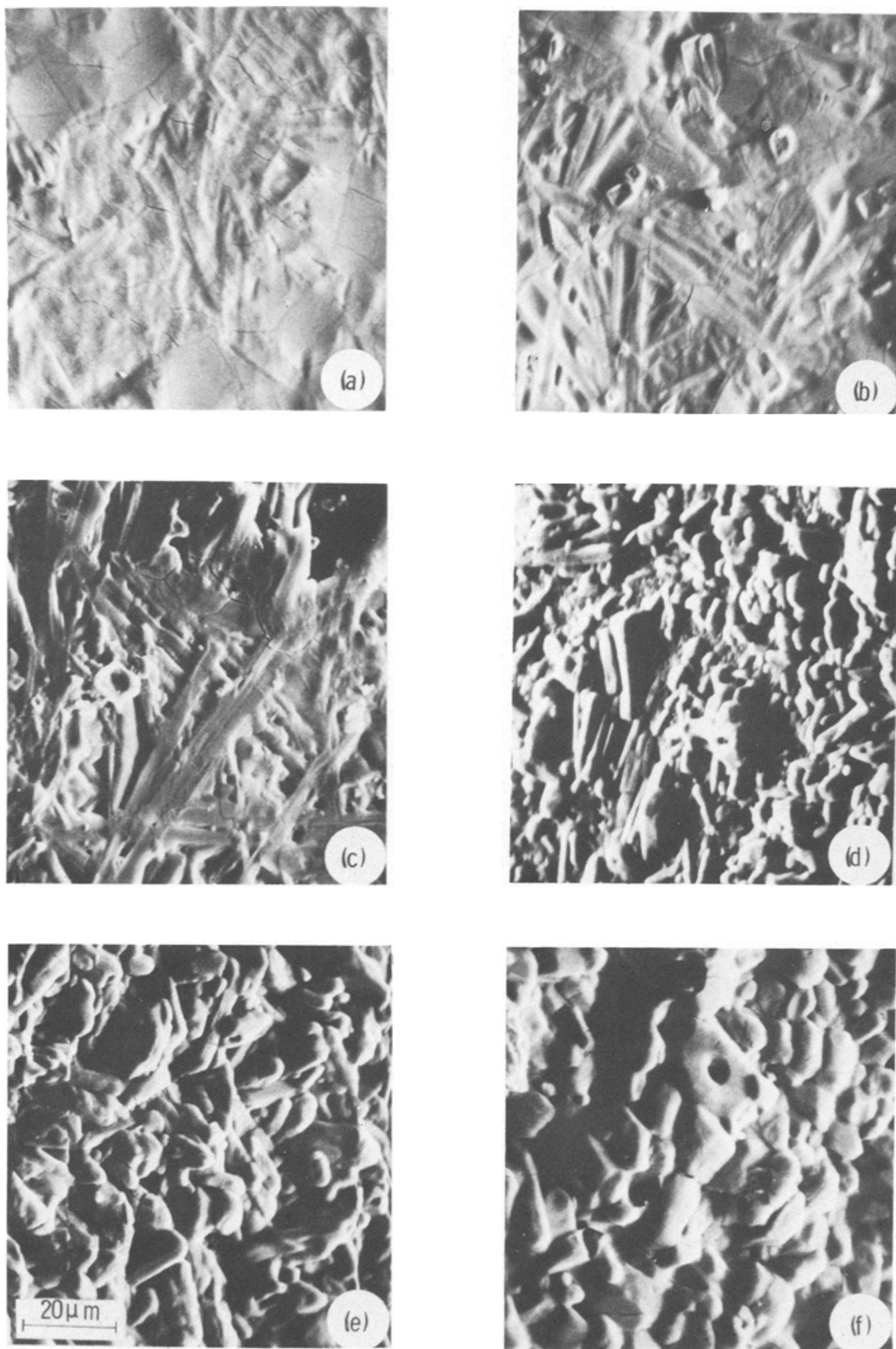

Figure 4 Scanning electron micrographs of surfaces of silicon nitride specimens oxidized for 30 h in oxygen at 1 atm pressure; (a) 982° C, (b) 1093° C, (c) 1205° C, (d) 1260° C, (e) 1305° C, (f) 1370° C.

scrapings from oxidized silicon nitride specimens. The unoxidized material contained predominantly β-Si_3N_4 with traces of Si_2ON_2. The amount of β-Si_3N_4 in the surface scrapings decreased as the amount of other phases increased with increasing temperature of oxidation, while the amount of Si_2ON_2 appeared to remain constant. The cristobalite (SiO_2) phase first appeared in specimens oxidized at 982° C, its amount increased in specimens oxidized at 1093 and 1205° C, and then levelled off in specimens oxidized at higher temperatures. Enstatite ($MgSiO_3$) and clino-enstatite

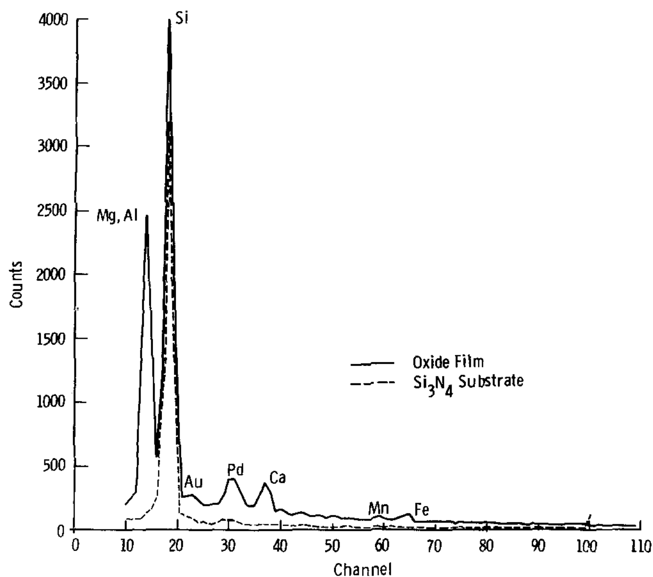

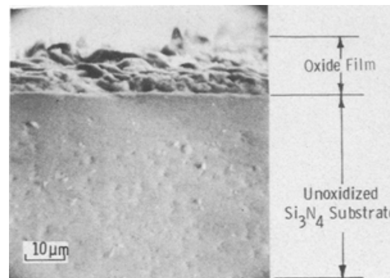

Figure 5 Scanning electron micrograph of the transverse section of Si_3N_4 specimen oxidized at 1260° C for 30 h in 1 atm oxygen, with energy dispersive X-ray analysis in the oxide layer and in Si_3N_4 substrate.

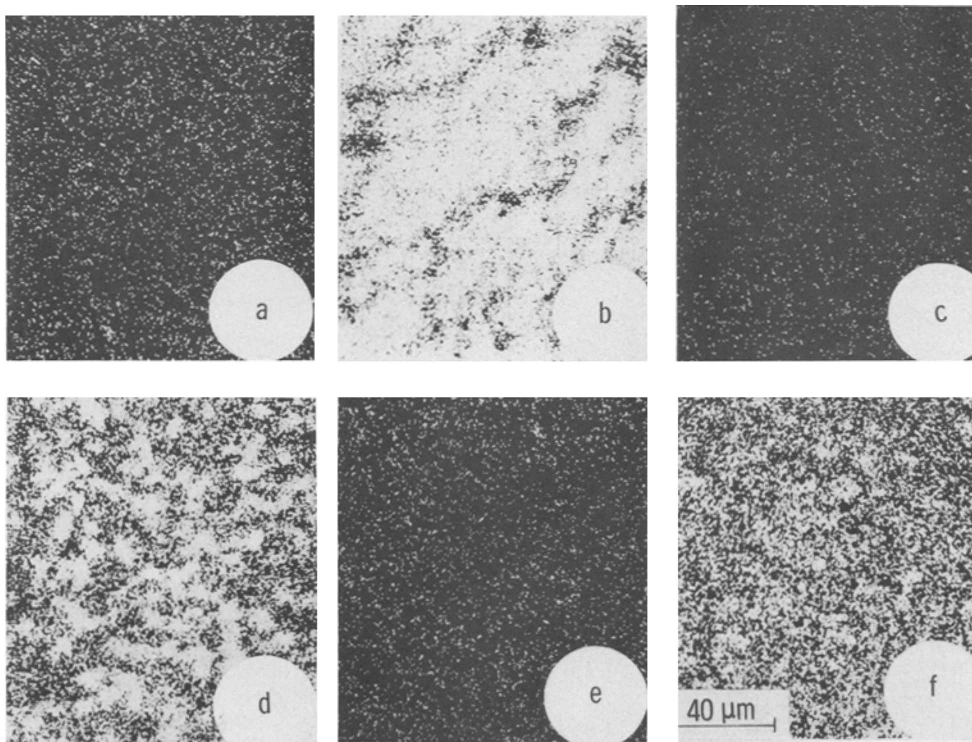

Figure 6 Scanning X-ray pictures showing concentrations of various elements in unoxidized Si_3N_4 and in the surface oxide on Si_3N_4; (a) Mg*K*α-unoxidized Si_3N_4; (b) Mg*K*α-oxide; (c) Ca*K*α-unoxidized Si_3N_4; (d) Ca*K*α-oxide; (e) Fe*K*α-unoxidized Si_3N_4; (f) Fe*K*α-oxide.

($MgSiO_3$) phases appeared in specimens oxidized at 1205° C and their amount increased with increasing temperature of oxidation.

The existence of cristobalite (crystalline SiO_2) at 982° C suggests that additive and impurity elements (mainly Mg and Ca) lower the devitrification temperature of silica glass by reducing its viscosity [10]. Even though X-ray diffraction analysis did

not detect any phases containing Ca, Na, K, Fe, Al and Mn, these elements were definitely present in surface oxide film as indicated by energy dispersive X-ray analysis and microprobe scans discussed earlier. These additive and impurity elements, therefore, must either form crystalline mixed silicates, such as diopside ($MgO \cdot CaO \cdot 2SiO_2$), with surface silica in amounts too small to be detectable by X-ray diffraction analysis, or they dissolve in surface silica to form an amorphous glassy phase. A mixed silicate phase, diopside ($MgO \cdot CaO \cdot 2SiO_2$), was detected in the present investigation in oxide film formed on Si_3N_4 after 4000h of oxidation at 1370° C. Mixed silicates like Mg(Ca, Fe)SiO_2 and $MgO \cdot CaO \cdot 2SiO_2$ have also been found [11] in oxide films formed on other hot-pressed Si_3N_4 materials containing much higher levels of impurities than the material used in the present investigation. This indicates that both the additive and impurity elements in hot-pressed Si_3N_4 form mixed silicates, e.g. diopside, in addition to enstatite in the oxide film.

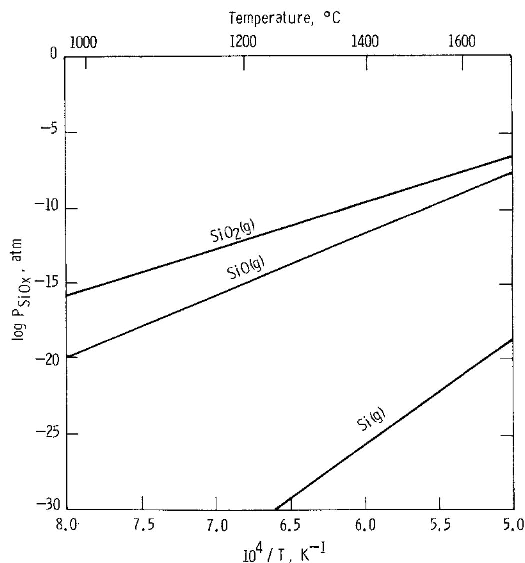

Figure 7 Partial pressures of various volatile species over SiO_2(s, l) in oxygen at 1 atm pressure.

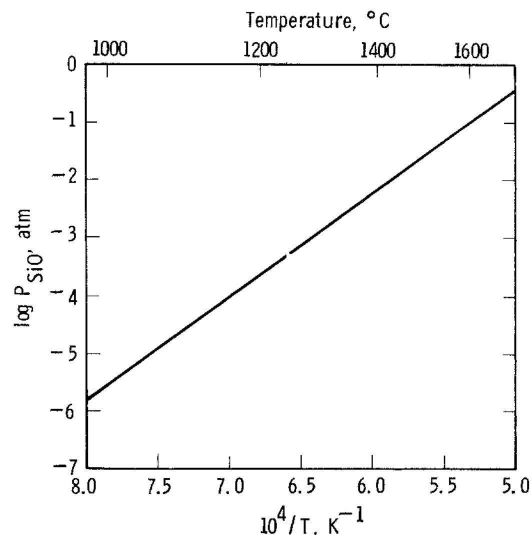

Figure 8 Equilibrium pressure of SiO(g) at Si_3N_4(s)–SiO_2(s) interface according to Reaction 2.

4. Discussion

4.1. Formation of volatile species

As discussed above, a passive film of SiO_2(s) is formed on the surface of Si_3N_4 in oxidizing atmospheres at elevated temperature, which subsequently reacts with additive and impurity elements to form various mixed silicates. However, for the sake of simplicity in considering the role of volatilization in oxidation of Si_3N_4, we would assume that the oxide film which forms on Si_3N_4 is predominantly SiO_2(s). The volatilization and/or decomposition of this surface SiO_2(s) could result in the formation of various volatile species. e.g. SiO_2(g), SiO(g) and Si(g). The theoretical partial pressures of these volatile species over SiO_2(s) in 1 atm oxygen pressure, calculated using thermochemical data from JANAF Tables [12], are shown in Fig. 7 as a function of temperature. The predominant volatile species over SiO_2(s) is seen to be SiO_2(g) with a partial pressure of less than 10^{-10} atm at 1400° C. The partial pressures of SiO(g) and Si(g) are even lower, and hence any loss in weight due to volatilization of surface SiO_2(s) can be ignored in the oxidation of Si_3N_4 in pure oxygen up to at least 1400° C. Thus the observed weight gains (Fig. 1) are not compensated by any volatilization weight loss.* The volatilization of surface SiO_2(s, l) could, however, become important in oxidation at higher temperatures and reduced oxygen partial pressures.

The SiO_2(s) formed at the surface of Si_3N_4 could also react at Si_3N_4(s)–SiO_2(s) interface to produce SiO(g) according to Reaction 2. The equilibrium partial pressures of SiO(g), which could thus form at Si_3N_4(s)–SiO_2(s) interface, have been calculated using thermodynamic data from available literature [12], and are shown in Fig. 8 as a function of temperature. At temperature up to

* However, there is a loss in weight due to formation and evolution of nitorgen so that the observed weight gain is only about 41% of the oxygen reacted.

1400° C, these SiO(g) pressures are not appreciable. Any SiO(g) formed at Si_3N_4(s)–SiO_2(s) interface should, however, be oxidized to SiO_2(s) in pores and fissures, which are formed by the evolution of N_2 by Reaction 1.

4.2. Phases formed by oxidation

In addition to Si and SiO_2, the generally recognized condensed phases in the silicon–nitrogen–oxygen system are α-Si_3N_4, β-Si_3N_4 and Si_2ON_2. For many years, the α- and β-forms of Si_3N_4 were thought to be low temperature and high temperature modifications, respectively, of the same compound [13, 14]. However, Wild *et al.* [15] suggested that β-Si_3N_4 is pure Si_3N_4 while α-Si_3N_4 is an oxynitride of silicon containing ~ 1 at.% oxygen with the approximate formula $Si_{11.4}N_{15}O_{0.3}$. Using the thermodynamic data of Wild *et al.* [16] for the formation of α-Si_3N_4, β-Si_3N_4 and Si_2ON_2, Jansson and Gulbransen [17] have constructed a thermochemical phase diagram for the Si–N–O system which is shown in Fig. 9. This diagram shows the stability regions of various condensed phases as a function of oxygen and nitrogen partial pressures. While the positions of the β-Si_3N_4/α-Si_3N_4 and α-Si_3N_4/Si_2ON_2 phase boundaries in this diagram are based solely on the data of Wild *et al.* [16], the positions of other phase boundaries are in good agreement with those calculated from other literature data [12, 18, 19].

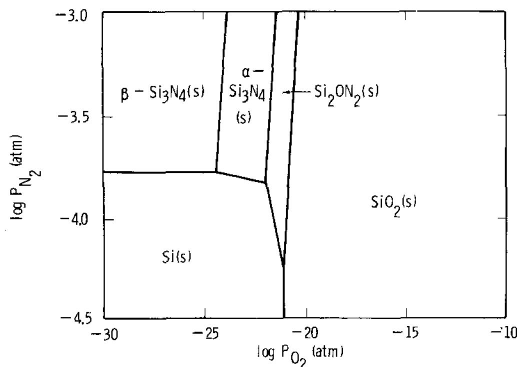

Figure 9 Thermochemical phase diagram for Si–N–O system at 1567 K based on the data of [16].

Based on this thermochemical diagram, one would expect that the oxidation of β-Si_3N_4 will result in the formation of a three-layered oxidation product consisting of α-Si_3N_4, Si_2ON_2 and SiO_2. In the present investigation, however, the oxide film was not found to be layered, and no α-Si_3N_4 was detected in the oxide film even at the highest temperature of oxidation. Thus even though it is possible that additive and impurity elements may have altered the expected three-layered nature of the oxide film, it also indicates that the thermochemical diagram shown in Fig. 9 could be in error. Priest *et al.* [20] and Kohatsu and McCauley [21] have recently shown that α-Si_3N_4 is not an oxynitride of silicon as suggested by Wild *et al.* [15, 16] but rather a true silicon nitride. Several discrepancies also exist [19] in the thermodynamic data for silicon oxynitride [17], and it is not completely certain that silicon oxynitide (Si_2ON_2) can exist as a pure compound by itself [22]. Thus there is a need for precise definition of various phases in the Si–N–O system and for their accurate thermodynamic properties before a complete understanding of the oxidation behaviour of silicon nitride can be achieved. The presence of additive and various impurity elements in hot-pressed form of silicon nitride further complicates the situation.

4.3 Processes occurring during oxidation

The parabolic nature of the rate curves indicates that the oxidation of hot-pressed silicon nitride is controlled by a diffusional mechanism. The many possible diffusional reactions which could occur during oxidation of hot-pressed Si_3N_4 are shown schematically in Fig. 10. As suggested by various authors [3, 5, 23–31] by experiments on the oxidation of Si, SiC and Si_3N_4, one would expect

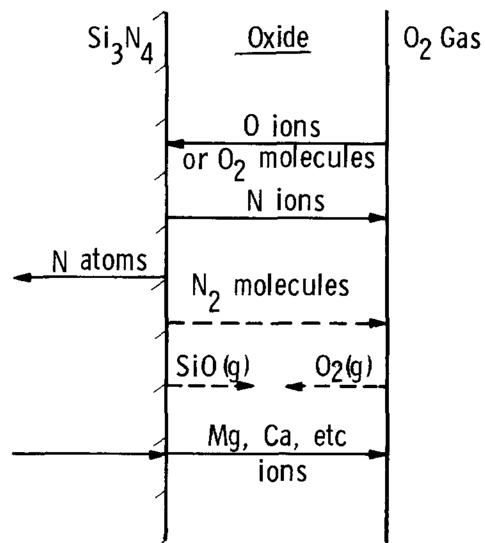

Figure 10 Schematic representation of varous reactions possible during oxidation of hot-pressed Si_3N_4. Dashed lines indicate transport in pores and fissures in the oxide film.

TABLE II Comparison of activation energies

System	Temperature range (° C)	Activation energy (kJ mol^{-1})	Reference
Hot-pressed Si_3N_4 in O_2	1000–1400	375	Present work
Powder Si_3N_4 in O_2	1065–1340	256	[3]
Powder Si_3N_4 in air	1065–1340	285	[3]
Powder Si_3N_4 in O_2 or air	1100–1300	147	[5]
Powder SiC in O_2	900–1600	65–85	[23]
Powder SiC in O_2	1300–1550	191	[24]
Powder SiC in O_2	1200–1500	277	[25]
Powder SiC in O_2	900–1300	210	[26]
Powder SiC in air	900–1300	336	[26]
Si in O_2	900–1200	125–130	[27–29]
O_2 diffusion in fused SiO_2	925–1225	298	[30]
O_2 diffusion in fused SiO_2	850–1250	122	[31]

the growth of the oxide layer on Si_3N_4 to occur by inward diffusion of oxygen ions or molecules. Table II lists the values of activation energies for the parabolic oxidation of Si, Si_3N_4 and SiC, which might be expected to show similar oxidation kinetics since SiO_2(s) is formed in all three cases. Even though there is wide variation in literature values of the activation energies, the activation energy of 375 kJ mol^{-1} for oxidation of hot-pressed Si_3N_4 determined in this investigation is still much higher than the highest value reported. A high value might be due to diffusion of oxygen ions or molecules through an oxide layer composed of not only silica, but also magnesium silicate and various mixed silicates such as diopside. Literature data are not available for oxygen diffusion in magnesium silicate or diopside for comparison of activation energies. But the fact that the activation energy is very high and the oxidation rate of hot-pressed silicon nitride is independent of oxygen partial pressure suggests that a diffusional mechanism other than inward oxygen ion diffusion is rate controlling, although this cannot be said with certainty.

One also has to account for nitrogen gas evolved at the Si_3N_4(s)–SiO_2(s) interface according to Reaction 1 in the oxidation of Si_3N_4. There are three processes, as shown in Fig. 10, by which this nitrogen gas may be removed from the interface. Firstly, nitrogen atoms may diffuse outwards through the oxide film and recombine at its surface to form N_2 molecules. Secondly, nitrogen can be removed from Si_3N_4(s)–oxide interface by inward diffusion of nitrogen into silicon nitride. The possibility and extent of this process depends upon the stoichiometry and diffusion rates in hot-pressed silicon nitride material. However, no data are available to further explore this process. The third process, which most probably occurs in the oxidation of hot-pressed silicon nitride, is the formation of N_2 bubbles at the Si_3N_4(s)–oxide interface. When nitrogen pressure within such bubbles exceeds the ambient pressure, the bubbles are released causing cracking of the oxide layer and forming of a pore network in it as seen in Fig. 4.

In addition to the transport of gaseous species as discussed above, one also has to account for the observed concentration of Mg, Ca, Fe, Al, etc., in the oxide film. It appears certain that during oxidation of Si_3N_4, these elements, which are predominantly present in a grain-boundary glass phase in the starting material, diffuse outwards from the grain boundaries. Thus, the diffusion of these cations outwards from the glass phase and through the oxide film may be the rate controlling process in the oxidation of hot-pressed silicon nitride. Considering the complexity of the system, the fact that a single straight line can be drawn on an Arrhenius type plot (Fig. 3) and a single value of activation energy obtained may be quite fortuitous. Even then, the high value of activation energy (375 kJ mol^{-1}) for oxidation of hot-pressed Si_3N_4 compares favourably with activation energies for cation (Mg^{2+}, Ca^{2+}) diffusion in oxides and silicates, e.g. 331 kJ mol^{-1} for Mg^{2+} diffusion in MgO [32], 281 kJ mol^{-1} for Mg^{2+} diffusion in Mg_2SiO_4 [33], and 376 to 397 kJ mol^{-1} for Ca^{2+} diffusion in several compositions in the CaO–SiO_2 system [34, 35]. Furthermore, the oxidation rate of hot-pressed silicon nitride has been found to increase with increasing amount of MgO additive, and also with increasing concentration of Ca, Na and K impurities [36]; and the oxidation rates of silicon nitride hot-pressed with different additives, e.g. MgO and

Y_2O_3, have been found to be widely different under same oxidation conditions [37]. Even though different rates of oxidation with different impurity levels and additives may be due to the formation of glassy phases with different viscosities, these evidences lend credence to the hypothesis that the oxidation of hot-pressed silicon nitride is controlled by the diffusion of additive and impurity cations (mainly Mg^{2+} and Ca^{2+}) from the grain-boundary glass phase through the surface oxide film.

A knowledge of the defect structure of the oxide formed and of the diffusion rates of various elements in it is necessary for a complete understanding of the oxidation behaviour of hot-pressed Si_3N_4. It also shows that the mechanism and kinetics of oxidation of hot-pressed silicon nitride may be significantly different than that for pure Si_3N_4 such as chemically vapour-deposited silicon nitride.

5. Conclusions

(1) The oxidation of hot-pressed Si_3N_4 in 1 atm oxygen follows classical parabolic behaviour with an activation energy of 375 kcal mol^{-1} in the temperature range 1000 to 1400° C.

(2) The oxidation rate is independent of ambient oxygen and nitrogen partial pressures.

(3) The oxide film formed consists of cristobalite, enstatite and possibly mixed silicates like diopside.

(4) Even though it cannot be determined unambiguously with the present data, the diffusion of Mg^{2+} and Ca^{2+} cations from the grain-boundary glass phase through the oxide film appears to be the rate controlling.

(5) A knowledge of the thermodynamic properties of the various phases in Si–N–O and other multicomponent systems involving additive and impurity elements, and of the diffusion rates in mixed silicates is required for a complete understanding of oxidation behaviour.

Acknowledgements

This work was supported by the Advanced Research Projects Agency, Department of Defense, under Contract No. DAAG 46-71-C-0162.

References

1. A. F. MCLEAN, E. A. FISHER and R. J. BRATTON, Report No. AMMRC 72-19, (1972).
2. J. J. BURKE, A. E. GORUM and R. N. KATZ, eds., "Ceramics for High Performance Applications" (Brook Hill, Chestnut Hill, 1974).
3. R. M. HORTON, *J. Amer. Ceram. Soc.* **52** (1969) 121.
4. D. TETARD, P. LORTHOLARY, P. GOURSAT and M. BILLY, *Rev. Int. Haut. Temp. Refrac.* **10** (1973) 153.
5. P. GOURSAT, P. LORTHOLARY, D. TETARD and M. BILLY, in Proceedings of the 7th International Symposium on Reactivity of Solids, Bristol (1972) p. 315.
6. A. G. EVANS and R. W. DAVIDGE, *J. Mater. Sci.* **5** (1970) 314.
7. C. WAGNER, *J. Appl. Phys.* **29** (1959) 305.
8. S. C. SINGHAL, in Proceedings of the 1974 Gas Turbine Materials in The Marine Environment Conference, edited by J. W. Fairbanks and I. Machlin, Battelle's Metals and Ceramics Information Center, Report 75-27, (1975) p. 311.
9. R. KOSSOWSKY, *J. Mater. Sci.* **8** (1973) 1603.
10. E. T. TURKDOGAN and P. M. BILLS, *Amer. Ceram. Soc. Bull.* **39** (1960) 682.
11. R. KOSSOWSKY, *J. Amer. Ceram. Soc.* **56** (1973) 531.
12. D. R. STULL and H. PROPHET, JANAF Thermochemical Tables, NSRDS-NBS 37, (1971).
13. W. D. FORGENG and B. F. DECKER, *Trans. Met. Soc. AIME* **212** (1958) 343.
14. S. N. RUDDLESDEN and P. POPPER, *Acta Cryst.* **11** (1958) 465.
15. S. WILD, P. GRIEVESON and K. H. JACK, "Special Ceramics" Vol. 5, edited by P. Popper (The British Ceramic Research Association, Stoke-on-Trent, 1972) p. 385.
16. *Idem, ibid* p. 271.
17. S. A. JANSSON and E. A. GULBRANSEN, in "High Temperature Gas–Metal Reactions in Mixed Environments", edited by S. A. Jansson and Z. A. Foroulis (TMS-AIME, New York, 1973).
18. W. R. RYALL and A. MUAN, *Science* **165** (1969) 1363.
19. H. SCHICK, "Thermodynamics of Certain Refractory Compounds", Vol. 2, (Academic Press, New York, 1966).
20. H. F. PRIEST, F. C. BURNS, G. L. PRIEST and E. C. SKAAR, *J. Amer. Ceram. Soc.* **56** (1973) 395.
21. I. KOHATSU and J. W. MCCAULEY, *Mat. Res. Bull.* **9** (1974) 917.
22. H. F. PRIEST, Army Materials and Mechanics Research Center, private communication (1974).
23. P. J. JORGENSEN, M. E. WADSWORTH and I. B. CUTLER, *J. Amer. Ceram. Soc.* **42** (1959) 613.
24. *Idem, ibid* **44** (1961) 258.
25. R. F. ADAMSKY, *J. Phys. Chem.* **63** (1959) 305.
26. G. ERVIN, *J. Amer. Ceram. Soc.* **41** (1958) 347.
27. F. W. AINGER, *J. Mater. Sci.* **1** (1966) 1.
28. B. E. DEAL, *J. Electrochem. Soc.* **110** (1963) 527.
29. H. C. EVITTS, H. W. COOPER and S. S. FLASCHEN, *J. Electrochem. Soc.* **111** (1964) 699.
30. E. W. SUCOV, *J. Amer. Ceram. Soc.* **46** (1963) 14.
31. E. L. WILLIAMS, *ibid* **48** (1965) 190.
32. R. LINDNER and G. PARFITT, *J. Chem. Phys.* **26** (1957) 182.
33. G. BORCHARDT and H. SCHMALZRIED, *Ber. Deut. Keram. Ges.* **49** (1972) 5.

34. V. A. MAJDIC and H. HENNING, *ibid* 47 (1970) 53.
35. B. V. VOLKONSKII and L. G. SUDAKAS, *Tsement* 23 (1957) 17.
36. R. KOSSOWSKY and S. C. SINGHAL, in "Grain Boundaries in Engineering Materials", edited by J. L. Walter, J. H. Westbrook and D. A. Woodford (Claitor's, Baton Rouge, 1975) p. 275.
37. S. C. SINGHAL, Westinghouse Research Labs, unpublished work (1975).

Received 7 April and accepted 5 September 1975.